



Cite this: *Nanoscale*, 2015, 7, 9894

Can graphene quantum dots cause DNA damage in cells?†

Dan Wang,^{‡a,c} Lin Zhu,^{‡b} Jian-Feng Chen^{*a} and Liming Dai^{*c}

Graphene quantum dots (GQDs) have attracted tremendous attention for biological applications. We report the first study on cytotoxicity and genotoxicity of GQDs to fibroblast cell lines (NIH-3T3 cells). The NIH-3T3 cells treated with GQDs at dosages over 50 $\mu\text{g mL}^{-1}$ showed no significant cytotoxicity. However, the GQD-treated NIH-3T3 cells exhibited an increased expression of proteins (p53, Rad 51, and OGG1) related to DNA damage compared with untreated cells, indicating the DNA damage caused by GQDs. The GQD-induced release of reactive oxygen species (ROS) was demonstrated to be responsible for the observed DNA damage. These findings should have important implications for future applications of GQDs in biological systems.

Received 17th March 2015,
Accepted 21st April 2015

DOI: 10.1039/c5nr01734c

www.rsc.org/nanoscale

Introduction

Graphene quantum dots (GQDs), which refer to graphene dots of smaller than 100 nm in size and less than 10 layers in thick-

ness, have emerged as a new class of carbon nanomaterials and attracted tremendous attention in recent years.^{1,2} The unique chemical/physical properties of GQDs make them attractive for various potential applications, ranging from energy to bio-related systems.^{3–9} In comparison with common semiconductor QDs (e.g., CdSe, CdTe, PbS),^{10–13} GQDs are mainly made up of carbon—the most abundant element in biological systems that is generally considered as an eco- and bio-friendly material.^{14,15} However, the biomedical applications of GQDs would hardly be realized unless the potential hazards of GQDs to human and other biological systems are carefully ascertained as some other carbon nanomaterials, including carbon nanotubes and nanodiamonds, have been demonstrated to cause DNA damage, though they showed no serious cytotoxicity at the cellular level.^{16,17}

^aState Key Laboratory of Organic–Inorganic Composites, Beijing University of Chemical Technology, Beijing 100029, China. E-mail: chenjf@mail.buct.edu.cn

^bInstitute of Advanced Materials for Nano-bio Applications, School of Ophthalmology and Optometry, Wenzhou Medical University, 270 Xueyuan Xi Road, Wenzhou, Zhejiang, China

^cCenter of Advanced Science and Engineering for Carbon (Case4Carbon), Department of Macromolecular Science and Engineering, Case School of Engineering, Case Western Reserve University, Cleveland, OH 44106, USA. E-mail: liming.dai@case.edu

†Electronic supplementary information (ESI) available. See DOI: 10.1039/c5nr01734c

‡These authors contributed equally to this work.



Dan Wang

Dan Wang is a postdoctoral fellow in the State Key Laboratory of Organic–Inorganic Composites, at the Beijing University of Chemical Technology. He received a B.Eng. degree in Materials Science and Engineering and a Ph.D. degree in Optical Engineering from Zhejiang University, in 2008 and 2013, respectively. Currently, he is a visiting scholar in Prof. Liming Dai's group at Case Western Reserve University. His

research interests focus on the synthesis, surface functionalization and bio-related applications of nanomaterials.



Lin Zhu

Lin Zhu is a Research Associate in the Institute of Advanced Materials for Nano-bio Applications, School of Ophthalmology and Optometry, Wenzhou Medical University. She received a B.S. degree in Medicine from Zhejiang Medical University and a PhD degree in Materials Science and Engineering from the University of Dayton. Her research interests focus on the functionalization and character-

ization of nanomaterials for bio-related applications, including cytotoxicity and genotoxicity of nanomaterials.

Recent studies on the *in vitro* and *in vivo* cytotoxicities of graphene-based materials have indicated that GQDs with a less than 50 nm side edge caused no obvious toxicity to a series of cell lines.^{18,19} For instance, Peng *et al.* found that nanosized graphene oxides did not lead to acute cytotoxicity to HeLa cells at a concentration of 40 $\mu\text{g mL}^{-1}$.²⁰ Li *et al.* observed no distinct cell death by incubating graphene oxide nanoparticles with AGS and HFF cells at a dose up to 100 $\mu\text{g mL}^{-1}$.²¹ Nurunnabi *et al.* performed *in vitro* cytotoxicity studies on carboxylated GQDs and observed no toxicity.²² These results from the cytotoxicity studies at the cellular level are in favor of GQDs for biomedical applications. Along with the cytotoxicity studies of GQDs, it is very important to evaluate the potential hazards of GQDs to DNA damage (*i.e.*, genotoxicity) because there is a close correlation between DNA damage and mutation or cancer. As far as we are aware, however, no genotoxicity study on GQDs has been reported.

A literature survey shows that some studies on cytotoxicity and genotoxicity of graphene oxides (GO) have been performed recently.^{23–26} For instance, Wang *et al.* reported significant cytotoxicity and genotoxicity of GO (200–500 nm) towards human lung fibroblast cells.²³ De Marzi and co-workers evaluated the size-dependent toxicity of GO *in vitro* for the A549, Caco-2 and Vero cell lines.²⁴ They observed a concentration-enhanced genotoxicity for micrometer-sized GO flakes (1320 nm), and a high degree of genotoxicity for nanometer-sized GO flakes (130 nm) at the lowest concentration tested.²⁴ Qiao *et al.* also reported that GO (2 μm in lateral size and 1.5 nm in thickness) caused DNA damage to human fibroblast cells at a very low concentration (1 $\mu\text{g mL}^{-1}$),²⁵ while Liu *et al.* observed mutagenesis induced by small sized GO both *in vitro* and *in vivo*.²⁶ As such, toxicity assessments of GQDs are critical because GQDs are similar in chemical structure with GO, but much smaller in size. More recently, Ge *et al.* demonstrated

that GQDs passivated with polyethylene glycol derivatives could generate reactive oxygen species (ROS) upon irradiation with light.²⁷ In view of the potential DNA damage caused by ROS, these studies prompted us to perform a systematic investigation of possible genotoxicity of GQDs using NIH-3T3 cells as a model system.

The NIH-3T3 cell line is one kind of fibroblast cell lines, which are among of the most common cells in animals and widely used for cytotoxicity and genotoxicity evaluations of nanomaterials.²⁸ In the present work, we synthesized GQDs through the oxidation of natural graphite with a commonly used chemical exfoliation (modified Hummer's) method.^{27,28} The genotoxicity of GQDs to NIH-3T3 cells was investigated by analysis of flow cytometry for the DNA damage related protein activation while the GQD-induced ROS generation was studied as a potential cause for the DNA damage. The cellular uptake of GQDs as well as cell death and proliferation of NIH-3T3 cells treated with GQDs were also studied to assess the cytotoxicity of GQDs.

Experimental

Preparation and characterization of GQDs

GQDs were synthesized by the oxidation of natural graphite following a modified Hummer's method.^{8,29,30} Briefly, 1 g graphite powders were added to 30 ml H_2SO_4 (98%) and the mixture solution was stirred for 10 h, followed by the addition of 6 g KMnO_4 into the solution while maintaining it at 10 °C. Thereafter, the solution was heated to 100 °C and stirred for 12 hours. Then, 150 mL DI water was added to dilute the solution, and 30 mL of 30% H_2O_2 was injected into the solution to completely react with the excess KMnO_4 . For purification, the resulting mixture was washed several times, first with 5% HCl



Jian-Feng Chen

Jian-Feng Chen is a Cheung Kong Distinguished Professor and Director of State Key Laboratory of Organic-Inorganic Composites, and Dean of the College of Chemical Engineering, Beijing University of Chemical Technology (China). He received a B.Eng. degree and a Ph.D. degree in Chemical Engineering from Zhejiang University in 1986 and 1992, respectively. He was a visiting full professor at Case Western Reserve University from

1997 to 1998. His research interests involve process intensification, nanomaterials and nanodrug delivery systems.



Liming Dai

Liming Dai is a Kent Hale Smith Professor in the Department of Macromolecular Science and Engineering at Case Western Reserve University. He is also director of the Center of Advanced Science and Engineering for Carbon (Case4Carbon). Before joining the CWRU, he was an associate professor of polymer engineering at the University of Akron and the Wright Brothers Institute Endowed Chair Professor at the University of

Dayton. He is a Fellow of the Royal Society of Chemistry and Fellow of the American Institute for Medical and Biological Engineering. His expertise covers the synthesis, functionalization and fabrication of conjugated polymers and carbon nanomaterials for energy- and bio-related applications.

solution and then with DI water. The obtained graphite oxide was dispersed in water and sonicated for 6 h. After that, the solution was filtered using a microporous membrane (0.22 μm). The filtrate containing GQDs was subsequently dialyzed in a 3.5 kDa cutoff cellulose membrane for several days. The final product of GQDs was collected by freeze drying treatment.

Transmission electron microscopy images were obtained using a TEM unit (JEOL JEM-1230) operating at 160 kV in bright-field mode. Atomic force microscopy images were recorded using a MultiMode scanning probe microscope (Veeco, USA) in a tapping mode with a scanning rate of 1 Hz. A Shimadzu UV 1800 scanning spectrophotometer and a HITACHI F-2500 fluorescence spectrophotometer were used to measure the absorption and photoluminescence spectra of samples, respectively. A PerkinElmer spectrum GX FTIR system was used to record the FTIR spectra of GQDs. The Raman spectra were collected using a Raman spectrometer (Renishaw) with a 514 nm laser. The thermogravimetric analysis (TGA) was performed using a TA Instrument with a heating rate of 10 $^{\circ}\text{C}$.

Cytotoxicity studies of GQDs

NIH-3T3 cells were cultured in a Dulbecco's minimum essential media (DMEM) with 10% fetal bovine serum (FBS), 1% penicillin, and 1% amphotericin B in flask. One day before the cell imaging experiments, NIH-3T3 cells were seeded in 35 mm cultivation dishes. Pre-determined amounts of GQD solutions were added to each of the wells on the plate to achieve a final concentration of 0, 5, and 50 $\mu\text{g mL}^{-1}$, respectively. After the GQD treatment for 3 and 24 h, the cells were washed three times with PBS (phosphate buffered saline, 1 \times) and imaged using a laser scanning confocal microscope (Olympus, FV 1000). Fluorescence imaging was performed under 405 nm laser excitation. The cytotoxicity of GQDs was assessed by the Cell Counting Kit-8 assay and MTT assay according to manufacturer's protocol. Typically, NIH-3T3 cells were incubated in culture media after incubation with GQDs at concentrations of 5 and 50 $\mu\text{g mL}^{-1}$ for 3 and 24 h, respectively. A multiwell spectrophotometer reader was used to measure the absorbance of each well at 450 nm. We assumed that the viability of control cells without the GQD treatment was 100%, and estimated the relative viability of cells treated with GQDs of various concentrations. The whole experiment was repeated 3 times and the results were averaged. For cell proliferation analysis, the average numbers of cells detached with 0.25% trypsin-EDTA were measured by using a Z1 Coulter Particle Counter (Beckman Coulter) at different time points after the sample treatment.

Cellular distribution of GQDs

For cellular distribution studies of GQDs, three groups of cells were treated with GQDs (50 $\mu\text{g mL}^{-1}$) at 37 $^{\circ}\text{C}$ for 2, 6 and 24 h, respectively. To investigate the possible pathway for GQD translocation, one group of cells was maintained at 4 $^{\circ}\text{C}$, followed by incubation with GQDs for 6 h. All the cells were washed three times with PBS (phosphate buffered saline, 1 \times)

and imaged using the laser scanning confocal microscope under 405 nm excitation.

Genotoxicity studies

NIH-3T3 cells were incubated in DMEM cell culture media with GQDs at concentrations of 0, 5, and 50 $\mu\text{g mL}^{-1}$. After incubation for 3 and 24 h, respectively, the cells were harvested and treated for flow cytometry following the manufactures protocol. To determine the expression level of p53 protein and Rad 51 protein, anti-p53 antibody and anti-Rad 51 antibody were simultaneously added into the samples. Flow cytometry studies were performed to analyze distributions of cells with green fluorescence and red fluorescence corresponding to the cells with p53 protein expression and Rad 51 expression, respectively. To determine the expression level of XRCC4 protein and OGG1 protein, anti-XRCC4 antibody and anti-OGG1 antibody were simultaneously added into the samples. Flow cytometry studies were performed to analyze distributions of cells with green fluorescence and red fluorescence corresponding to the cells with XRCC4 protein expression and OGG1 expression, respectively. The whole experiment was repeated 3 times.

Reactive oxygen species (ROS) generation

For the ROS assay-DCFH-DA, NIH-3T3 cells were seeded at a density of $150 \times 10^3 \text{ mL}^{-1}$ in black 96 well plates for 24 h. 200 μL of 100 μM DCFH-DA (Sigma) (in culture medium) was added to each well and incubated at 37 $^{\circ}\text{C}$ and 5% CO_2 culture conditions for 30 min. After the aspiration of the DCFH-DA, 200 μL of a dosing solution (1, 5, 10, 25 $\mu\text{g mL}^{-1}$) was added to each well. The plate was covered with aluminum foil to block light and placed in an incubator for 24 h. The intensity of the ROS probe was measured at 0 min and 24 h on a spectrophotometer (Molecular Devices, SpectraMax M2, SoftMax Pro 4.8, USA) with excitation at 485 nm, absorbance at 538 nm and a peak at 530 nm, following the manufacturer's procedure. We assumed that the ROS production of control cells is 0, and estimated the relative ROS production of cells treated with various GQDs (1, 5, 10, 25 $\mu\text{g mL}^{-1}$). The data are presented as the average ROS intensity at 24 h subtracted 0 min background intensity from 6 experiments with the standard deviation.

Results and discussion

To date, various synthetic approaches have been developed for the preparation of GQDs. Different synthetic methods often lead to GQDs with different sizes, functional groups, and optical properties. In this study, we examined the toxicity of GQDs synthesized by the oxidation of natural graphite according to a modified Hummer's method,^{27,28} which is generally considered as a promising approach for low-cost and large-scale production of GQDs.^{29,30} The morphology of the as-synthesized GQDs was characterized by TEM and AFM. A typical

TEM image of the resulting GQDs given in Fig. 1a shows an average lateral size of 40 nm. The corresponding AFM image with the height profile given in Fig. 1b reveals an average thickness of *ca.* 2 nm, indicating a few-layered graphene. Fig. 1c shows the absorbance and fluorescence spectra of an aqueous dispersion of GQDs. As shown in Fig. 1c, a distinct absorption peak at 230 nm due to the $\pi-\pi^*$ transition of C-C and C=C bonds in the sp^2 hybrid regions is evident, along with a relatively broad absorption band centered over 250 nm arising from the $\pi-\pi$ conjugation in GQDs. The fluorescence spectrum of GQDs under excitation of the 230 nm (absorption peak wavelength) UV light was measured with a peak at 410. Excitation-wavelength-dependent emission spectra were observed from the excitation-emission map shown in Fig. S1,[†] which shows that the maximum of the emission red-shifts with increasing the excitation wavelength. These results are similar to many previous reports on the fluorescence spectra of GQDs.^{3,31-33} The FTIR spectrum of the GQDs is reproduced in Fig. 1d, which shows the presence of oxygen-containing functional groups to render the GQDs soluble in water. Fig. 1e shows a typical Raman spectrum of GQDs, in which the D band at 1355 cm^{-1} and the G band at 1575 cm^{-1} were clearly observed with the peak intensity ratio (I_D/I_G) of 0.96 in consistency with the rich edge defects. Thermalgravimetric analysis

(TGA) of the GQDs in air reveals an initial $\sim 20\%$ weight loss up to $\sim 200\text{ }^\circ\text{C}$ attributable to the thermal desorption of water molecules physically adsorbed onto the hydrophilic GQD surface. The subsequent weight loss over $200\text{--}500\text{ }^\circ\text{C}$ probably originated from the loss of those chemically attached oxygen-containing groups (*e.g.*, $-\text{COOH}$ groups at the edge, $-\text{OH}$ groups on the basal plane) prior to the material decomposition at $600\text{ }^\circ\text{C}$. These results are consistent with those of GQDs previously reported in the literature.^{8,28,34,35}

The *in vitro* cytotoxicities of GQDs to NIH-3T3 cells were evaluated in terms of both the cell death and cell proliferation. MTT was used to study the cell viability for cells treated with various concentrations of GQDs at various times. As shown in Fig. 2a, no significant cell death was observed after the GQD treatment for either 3 or 24 hours, indicating low cytotoxicities for GQDs. This is also supported by a cell proliferation assay, in which the addition of GQDs ($5, 50\text{ }\mu\text{g mL}^{-1}$) caused no difference in the NIH-3T3 cell proliferation, compared with the control cells without the addition of GQDs (Fig. 2b). These results suggest that the GQDs are highly biocompatible at the cellular level.

The cellular distribution of GQDs was confirmed by laser scanning confocal fluorescence imaging. As can be seen in Fig. 3, the fluorescence emission intensity from NIH-3T3 cells incubated with GQDs at $37\text{ }^\circ\text{C}$ increased with increasing incubation time, indicating a time-dependent uptake of GQDs by the cells while control cells showed no obvious fluorescence. 3-D confocal imaging of the cells treated with GQDs showed that the fluorescence signal was present throughout the cells, confirming the internalization of GQDs (Fig. S2[†]). We also

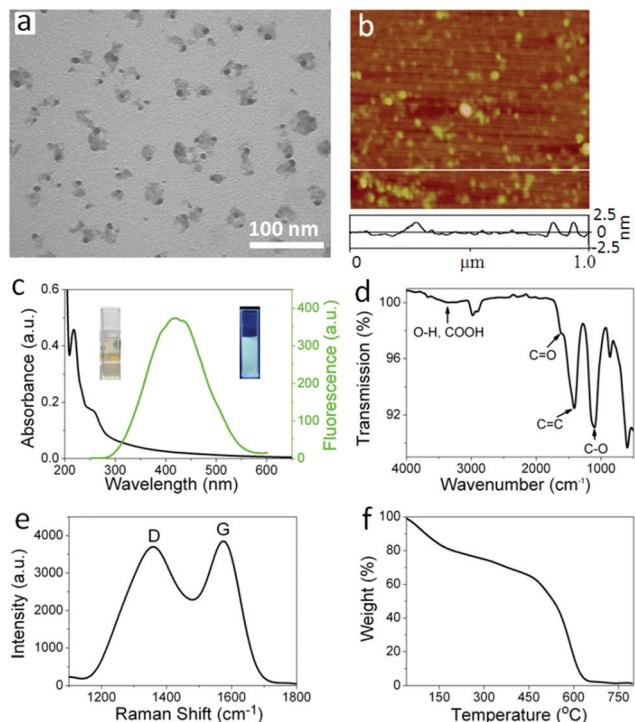


Fig. 1 (a) A TEM image of the as-synthesized GQDs; (b) an AFM image of the GQDs; (c) absorbance spectrum (black curve) and fluorescence spectrum (green curve, $\lambda_{\text{EX}} = 230\text{ nm}$) of an aqueous dispersion of GQDs (Inset: photos of an aqueous dispersion of GQDs under daylight lamp irradiation (left) and UV lamp excitation (right)). (d) FTIR spectrum of the GQDs; (e) Raman spectra of the GQDs; (f) TGA curve of the GQDs in air.

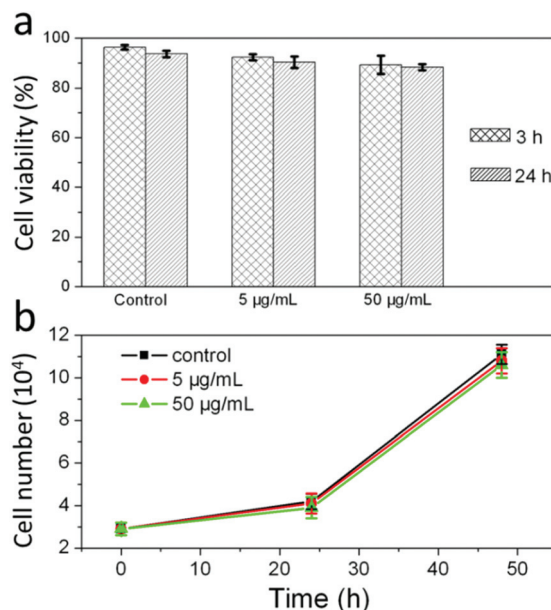


Fig. 2 (a) Cell viabilities of NIH-3T3 cells studied by using the MTT method and the cells were treated in cell culture media with GQDs ($0, 5$ and $50\text{ }\mu\text{g mL}^{-1}$) for 3 and 24 h, respectively. (b) Average numbers of NIH-3T3 cells after the addition of GQDs for 0, 24, and 48 h post incubation.

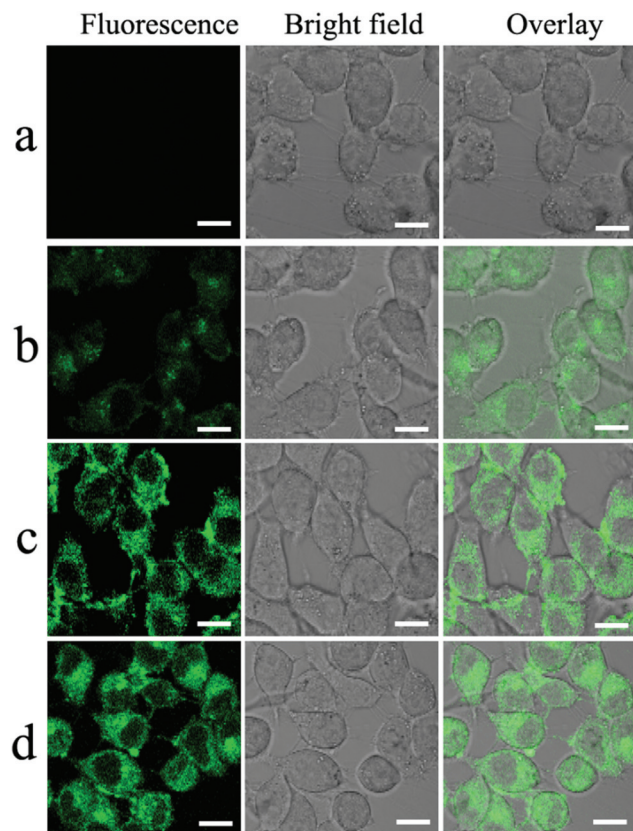


Fig. 3 Fluorescence images of (a) control cells and (b, c, d) cells treated with GQDs for 2, 6 and 24 h at 37 °C, respectively. Scale bar: 20 μm .

noted that the fluorescence of GQDs was observable from cells incubated with GQDs at 4 °C (Fig. S3†), even when the endocytosis of cells was completely blocked at such a low temperature.^{36,37} These results suggest that the cellular uptake of GQDs possibly relies on the direct penetration of cell membranes, rather than energy-dependent pathways (*e.g.*, endocytosis), in consistence with previous studies on the cellular uptake of graphene oxides and carbon nanotubes.^{20,37–39} There have been some controversies over the cellular distribution of GQDs. Several studies have demonstrated that GQDs can enter the cell nucleus^{40,41} while others reported the distribution of GQDs in the cytoplasm.^{6,22,42,43} The reported different distribution behaviours could come from differences in the surface functional groups and types of cell lines. Based on our fluorescence imaging, we believe that the GQDs are mainly located in the cytoplasm of NIH-3T3 cells. Nevertheless, it is known that DNA damage caused by a direct contact with nanoparticles through nuclear entry is one, but not the only possibility for nanoparticles to cause DNA damage, and that DNA damage can also be caused by indirect mechanisms through, for example, the interactions of DNA with ROS generated by nanoparticles in the cytoplasm.^{16,17,44,45}

Many biological methods, including Ames assay, comet assay, DNA fragmentation test, have been used for the evaluation of genotoxicity,^{44,45} along with some novel

approaches.^{46–48} Flow cytometry analysis has also been used as a powerful tool for the detection of DNA damage in cells.^{49–51} To investigate the possible DNA damage caused by GQDs, we monitored the expression levels of p53 and Rad 51 proteins in response to the GQD treatment by staining the cells with the respective fluorochromes, followed by flow cytometry analysis. The p53 protein is a tumor suppressor protein that remains inactive under normal conditions, which can activate DNA repair when DNA damage occurs. On the other hand, the Rad 51 protein plays a major role in the homologous recombination of DNA during double strand break repair. Enhanced expressions of these two proteins are often seen during the DNA damage. In the present study, a fluorescence activated cell sorter was used to investigate the p53 and Rad 51 expressions of NIH-3T3 cells incubated with GQDs at various concentrations. The cell cycle distributions were analyzed after the treatment of NIH-3T3 cells with GQDs and the subsequent addition of various antibodies, such as anti-p53 antibody and anti-Rad 51 antibody. Fig. 4a and b indicate that the treatment of GQDs and antibodies caused no significant cytotoxicity to cells, which allows us to further analyze the expressions of DNA damage related proteins in live cells. The DNA-damage-related protein intensity in the cell cycle is described using a density distribution by plotting the protein intensity along with the *x*-axis and the density of cells having the respective protein expression along the *y*-axis (Fig. 4c and d). Fig. 4c clearly shows that the GQD treatments at 5 and 50 $\mu\text{g mL}^{-1}$ induced an aberrant increase of p53 expression along with a concomitant increase in the cell density during a short time (3 h). As can be seen in Fig. 4c, a prolonged incubation (24 h) caused an increase in the p53 expression, but no obvious increase in the density of cells with p53 expression, indicating an increased DNA damage for a somewhat constant number of cells having the p53 protein expression. Similar trends were also observed for Rad 51 protein from the NIH-3T3 cells treated with GQDs (Fig. 4d). Therefore, these results clearly indicate the occurrence of DNA damage caused by GQDs.

In addition to p53 protein and Rad 51 protein, we also studied the expression of other DNA damage related proteins, including OGG1 protein and XRCC4 protein. OGG1 is the primary enzyme responsible for the excision of 8-oxoguanine (8-oxoG), a mutagenic base by-product that occurs as a result of exposure to ROS.¹⁶ XRCC4 is one of the several core proteins involved in the non-homologous end joining pathway to repair DNA double strand breaks (DSBs), which is the most harmful type of DNA damage. Once again, Fig. 5a and b indicate that the treatment of GQDs and antibodies caused no significant cytotoxicity to cells. However, Fig. 5c shows the enhanced expression of OGG1 protein, in similar expression patterns to those for p53 and Rad 51 expressions. It was noted that on the right panel of Fig. 5c, the cell density slightly decreased with the increase in OGG1 intensity, which was attributed to the cell death. However, the GQD treatments caused no significant change in the XRCC4 expression (Fig. 5d). Since the GQDs are mainly distributed in the cytoplasm of NIH-3T3 cells without direct contact with DNA in the nucleus (Fig. 3), the ROS gene-

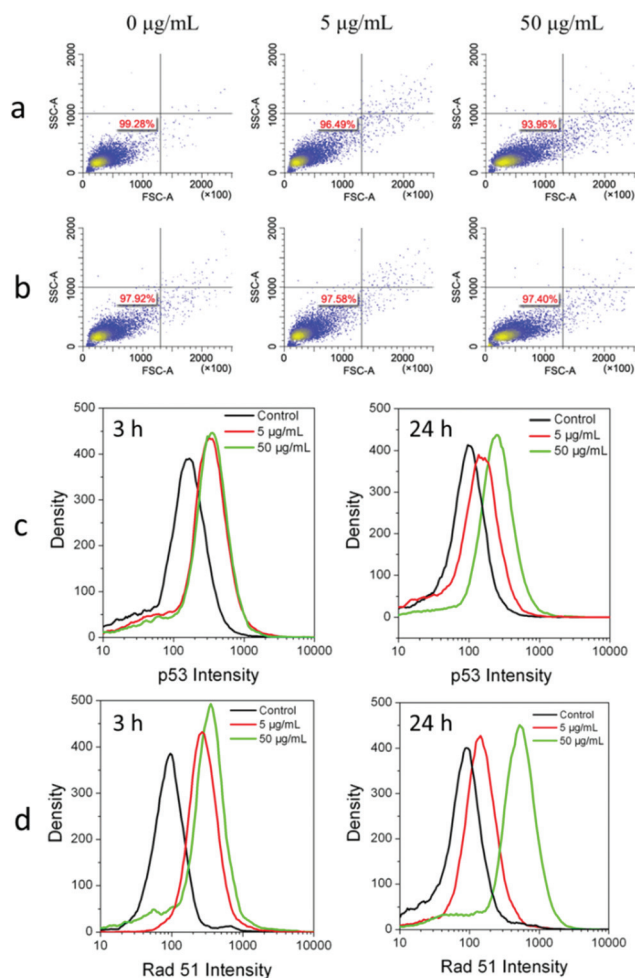


Fig. 4 Flow cytometry results of NIH-3T3 cells after (a) 3 h and (b) 24 h incubation with GQDs (0, 5, and 50 $\mu\text{g mL}^{-1}$) and then treated with anti-p53 antibody and anti-Rad 51 antibody, respectively; cell cycle phase-specific densities of p53 protein (c) and Rad 51 protein (d) intensity for different doses (0, 5, 50 $\mu\text{g mL}^{-1}$) of GQDs after 3 and 24 h incubation, respectively.

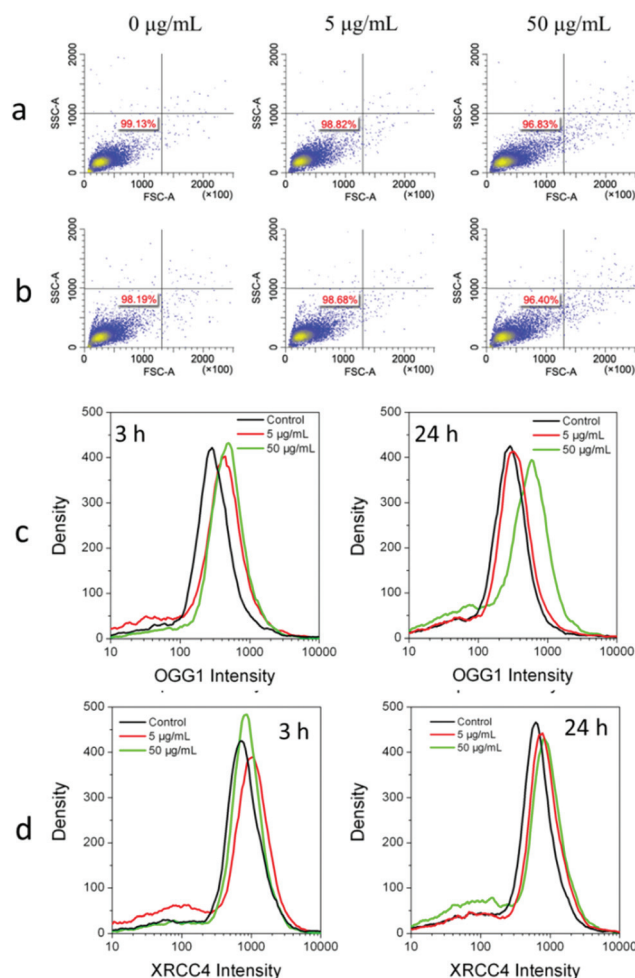


Fig. 5 Flow cytometry results for NIH-3T3 cells after (a) 3 h and (b) 24 h incubation with GQDs (0, 5, and 50 $\mu\text{g mL}^{-1}$), and then treated with anti-OGG1 antibody and anti-XRCC4 antibody, respectively; cell cycle phase-specific densities of OGG1 protein (c) and XRCC4 protein (d) for different doses (0, 5, 50 $\mu\text{g mL}^{-1}$) of GQDs after 3 and 24 h incubation, respectively.

ration is, most likely, responsible for the GQD-induced DNA damage in NIH-3T3 cells.^{16,17,44,45}

To confirm the ROS generation of NIH-3T3 cells treated with GQDs, the ROS assay-DCFH-DA measurement³⁶ was performed. Fig. 6 clearly shows that the treatment of NIH-3T3 cells with GQDs caused an increased ROS generation with respect to the control cells. Therefore, the DNA damage of NIH-3T3 cells could be caused by the GQD-induced ROS generation. Since graphene oxides have been reported to induce intracellular ROS generation in cells,²³ we compared the ROS generation level of NIH-3T3 cells incubated with GQDs and graphene oxides (0.5–5 μm), respectively, at the same concentration of 25 $\mu\text{g mL}^{-1}$. The results showed that GQDs induced lower ROS generation of cells than graphene oxides, indicating a better biocompatibility for the former. However, our results from the genotoxicity study of GQDs suggest that some cau-

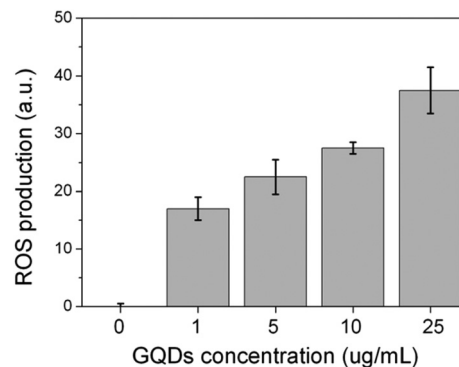


Fig. 6 ROS generation in NIH-3T3 cells after incubation with GQDs for 24 h. The data represent the average of six experiments with the standard deviation. Doses are 0 for the control and 1, 5, 10, and 25 $\mu\text{g mL}^{-1}$ for GQD treated groups.

tions are needed for the practical use of QGDs, though they are highly biocompatible at the cellular level.

Conclusions

QGDs have attracted much attention as a class of emerging materials for applications in many fields. Of particular interest, QGDs are promising for many biomedical applications (e.g., imaging, drug delivery). However, the studies on genotoxicity of QGDs are rarely reported. In this paper, we have demonstrated for the first time that QGDs can cause DNA damage in NIH-3T3 cells, though no obvious toxicity was observed at the cellular level. The QGD-induced DNA damage was indicated by an increased expression of proteins (p53, Rad 51, and OGG1) related to DNA damage compared with untreated cells. Although the QGDs were mainly distributed in the cytoplasm of the cells without direct contact with DNA, the QGD-induced ROS release was demonstrated to be responsible for the observed DNA damage. Our preliminary findings based on the systematic flow cytometry and ROS measurements suggest that a careful scrutiny of the genotoxicity of QGDs is needed even though they show no obvious toxicity at the cellular level. More biological assessments, including Ames assay, comet assay, and DNA fragmentation test, and cell cycle arrest study are helpful to understand the mechanism of DNA damage caused by QGDs, which should be good topics for future studies.

Acknowledgements

We are grateful for financial support from NSF (CMMI-1400274, CMMI-1266295), DAGSI (RQ20-CWRU-13-4), DOD-Army (W911NF-11-1-0209), WMU, and partial support from the open-funding program of State Key Laboratory of Organic-Inorganic Composites.

Notes and references

- Z. P. Zhang, J. Zhang, N. Chen and L. Qu, *Energy Environ. Sci.*, 2012, **5**, 8869–8890.
- L. Li, G. Wu, G. Yang, J. Peng, J. Zhao and J.-J. Zhu, *Nanoscale*, 2013, **5**, 4015–4039.
- Y. Li, Y. Hu, Y. Zhao, G. Shi, L. Deng, Y. Hou and L. Qu, *Adv. Mater.*, 2011, **23**, 776–780.
- X. Yan, X. Cui, B. Li and L. Li, *Nano Lett.*, 2010, **10**, 1869–1873.
- L. Chen, C. X. Guo, Q. Zhang, Y. Lei, J. Xie, S. Ee, G. Guai, Q. Song and C. M. Li, *ACS Appl. Mater. Interfaces*, 2013, **5**, 2047–2052.
- J. Peng, W. Gao, B. K. Gupta, Z. Liu, R. A. Rebeca, L. H. Ge, L. Song, L. B. Alemany, X. B. Zhan, G. H. Gao, S. A. Vithayathil, B. A. Kaiparettu, A. A. Marti, T. Hayashi, J. J. Zhu and P. M. Ajayan, *Nano Lett.*, 2012, **12**, 844–849.
- M. Nurunnabi, Z. Khatun, G. R. Reeck, D. Y. Lee and Y. K. Lee, *Chem. Commun.*, 2013, **49**, 5079–5081.
- J. Qian, D. Wang, F.-H. Cai, W. Xi, L. Peng, Z.-F. Zhu, H. He, M.-L. Hu and S. He, *Angew. Chem., Int. Ed.*, 2012, **51**, 10570–10575.
- X. T. Zheng, A. Than, A. Ananthanaraya, D. H. Kim and P. Chen, *ACS Nano*, 2013, **7**, 6278–6286.
- P. Alivisatos, *Nat. Biotechnol.*, 2004, **22**, 47–52.
- X. H. Gao, Y. Y. Cui, R. M. Levenson, L. W. K. Chung and S. M. Nie, *Nat. Biotechnol.*, 2004, **22**, 969–976.
- D. Wang, J. Qian, F. Cai, S. He, S. Han and Y. Mu, *Nanotechnology*, 2012, **23**, 245701.
- K. T. Yong, W. C. Law, R. Hu, L. Ye, L. W. Liu, M. T. Swihart and P. N. Prasad, *Chem. Soc. Rev.*, 2013, **42**, 1236–1250.
- L. Z. Feng and Z. A. Liu, *Nanomedicine*, 2011, **6**, 317–324.
- A. B. Seabra, A. J. Paula, R. de Lima, O. L. Alves and N. Duran, *Chem. Res. Toxicol.*, 2014, **27**, 159–168.
- L. Zhu, D. W. Chang, L. Dai and Y. Hong, *Nano Lett.*, 2007, **7**, 3592–3597.
- Y. Xing, W. Xiong, L. Zhu, E. Ōsawa, S. Hussin and L. Dai, *ACS Nano*, 2011, **5**, 2376–2384.
- Z. Liu, J. T. Robinson, X. Sun and H. Dai, *J. Am. Chem. Soc.*, 2008, **130**, 10876–10877.
- H. Zhang, G. Gruener and Y. Zhao, *J. Mater. Chem. B*, 2013, **1**, 2542–2567.
- C. Peng, W. Hu, Y. Zhou, C. Fan and Q. Huang, *Small*, 2010, **6**, 1686–1692.
- J. L. Li, H. C. Bao, X. L. Hou, L. Sun, X. G. Wang and M. Gu, *Angew. Chem., Int. Ed.*, 2012, **51**, 1830–1834.
- M. Nurunnabi, Z. Khatun, K. M. Huh, S. Y. Park, D. Y. Lee, K. J. Cho and Y. K. Lee, *ACS Nano*, 2013, **7**, 6858–6867.
- A. Wang, K. Pu, B. Dong, Y. Liu, L. Zhang, Z. Zhang, W. Duan and Y. Zhu, *J. Appl. Toxicol.*, 2013, **33**, 1156–1164.
- L. De Marzi, L. Ottaviano, F. Perrozzi, M. Nardone, S. Santucci, J. De Lapuente, M. Borrás, E. Treossi, V. Palermo and A. Poma, *J. Biol. Regul. Homeost. Agents*, 2013, **28**, 281–289.
- Y. Qiao, J. An and L. Ma, *Anal. Chem.*, 2013, **85**, 4107–4112.
- Y. Liu, Y. Luo, J. Wu, Y. Wang, X. Yang, R. Yang, B. Wang, J. Yang and N. Zhang, *Sci. Rep.*, 2013, **3**, 3469.
- J. Ge, M. Lan, B. Zhou, W. Liu, L. Guo, H. Wang, Q. Jia, G. Niu, X. Huang, H. Zhou, X. Meng, P. Wang, C.-S. Lee, W. Zhang and X. Han, *Nat. Commun.*, 2014, **5**, 4596.
- E. Demir, H. Akça, B. Kaya, D. Burgucu, O. Tokgün, F. Turna, S. Aksakal, G. Vales, A. Creus and R. Marcos, *J. Hazard. Mater.*, 2014, **264**, 420–429.
- W. S. Hummers and R. E. Offeman, *J. Am. Chem. Soc.*, 1958, **80**, 1339.
- Y. Sun, S. Wang, C. Li, P. Luo, L. Tao, Y. Wei and G. Shi, *Phys. Chem. Chem. Phys.*, 2013, **15**, 9907–9913.
- G. S. Kumar, R. Roy, D. Sen, U. K. Ghorai, R. Thapa, N. Mazumder, S. Saha and K. K. Chattopadhyay, *Nanoscale*, 2014, **6**, 3384–3391.
- Y. H. Li, L. Zhang, J. Huang, R. P. Liang and J. D. Qiu, *Chem. Commun.*, 2013, **49**, 5180–5182.

- 33 V. Gupta, N. Chaudhary, R. Srivastava, G. D. Sharma, R. Bhardwaj and S. Chand, *J. Am. Chem. Soc.*, 2011, **133**, 9960–9963.
- 34 D. Y. Pan, J. C. Zhang, Z. Li and M. H. Wu, *Adv. Mater.*, 2010, **22**, 734–738.
- 35 R. Q. Ye, C. S. Xiang, J. Lin, Z. W. Peng, K. W. Huang, Z. Yan, N. P. Cook, E. L. G. Samuel, C. C. Hwang, G. D. Ruan, G. Ceriotti, A. R. O. Raji, A. A. Marti and J. M. Tour, *Nat. Commun.*, 2013, **4**, 2943.
- 36 A. Aranda, L. Sequedo, L. Tolosa, G. Quintas, E. Burello, J. V. Castell and L. Gombau, *Toxicol. in Vitro*, 2013, **27**, 954–963.
- 37 F. Zhou, D. Xing, B. Wu, S. Wu, Z. Ou and W. R. Chen, *Nano Lett.*, 2010, **10**, 1677–1681.
- 38 D. Pantarotto, J. P. Briand, M. Prato and A. Bianco, *Chem. Commun.*, 2004, 16–17.
- 39 A. E. Porter, M. Gass, K. Muller, J. N. Skepper, P. A. Midgley and M. Welland, *Nat. Nanotechnol.*, 2007, **2**, 713–717.
- 40 C. Wang, C. Wu, X. Zhou, T. Han, X. Xin, J. Wu, J. Zhang and S. Guo, *Sci. Rep.*, 2013, **3**, 2852.
- 41 C. Wu, C. Wang, T. Han, X. Zhou, S. Guo and J. Zhang, *Adv. Healthcare Mater.*, 2013, **2**, 1613–1619.
- 42 S. Zhu, J. Zhang, S. Tang, C. Qiao, L. Wang, H. Wang, X. Liu, B. Li, Y. Li, W. Yu, X. Wang, H. Sun and B. Yang, *Adv. Funct. Mater.*, 2012, **22**, 4732–4740.
- 43 X. Wang, X. Sun, J. Lao, H. He, T. Cheng, M. Wang, S. Wang and F. Huang, *Colloids Surf., B*, 2014, **122**, 638–644.
- 44 Z. Magdolenova, A. Collins, A. Kumar, A. Dhawan, V. Stone and M. Dusinska, *Nanotoxicology*, 2014, **8**, 233–278.
- 45 N. Golbamaki, B. Rasulev, A. Cassano, R. L. Marchese Robinson, E. Benfenati, J. Leszczynski and M. T. D. Cronin, *Nanoscale*, 2015, **7**, 2154–2198.
- 46 W. Wei, J. Zhou, H. Li, L. Yin, Y. Pu and S. Liu, *Analyst*, 2013, **138**, 3253–3258.
- 47 J. Qian, C. Zhang, X. Cao and S. Liu, *Anal. Chem.*, 2010, **82**, 6422–6429.
- 48 J. Qian, H. C. Dai, X. H. Pan and S. Q. Liu, *Biosens. Bioelectron.*, 2011, **28**, 314–319.
- 49 F. Bunz, A. Dutriaux, C. Lengauer, T. Waldman, S. Zhou, J. P. Brown, J. M. Sedivy, K. W. Kinzler and B. Vogelstein, *Science*, 1998, **282**, 1497–1501.
- 50 L. J. Chappell, M. K. Whalen, S. Gurai, A. Ponomarev, F. A. Cucinotta and J. M. Pluth, *Radiat. Res.*, 2010, **174**, 691–702.
- 51 Z. Darzynkiewicz, X. Huang and M. Okafuji, *Methods Mol. Biol.*, 2006, **314**, 81–93.